Journal Pre-proof


# Conditional distribution selection for SPEI-daily and its revealed meteorological drought characteristics in China from 1961 to 2017

Bin Ma, Bo Zhang, Lige Jia, Hao Huang

PII: S0169-8095(19)30945-7

DOI: https://doi.org/10.1016/j.atmosres.2020.105108

Reference: ATMOS 105108

To appear in: *Atmospheric Research*

Received date: 21 July 2019

Revised date: 10 June 2020

Accepted date: 10 June 2020

Please cite this article as: B. Ma, B. Zhang, L. Jia, et al., Conditional distribution selection for SPEI-daily and its revealed meteorological drought characteristics in China from 1961 to 2017, *Atmospheric Research* (2020), https://doi.org/10.1016/j.atmosres.2020.105108

# Conditional Distribution Selection for SPEI-daily and Its Revealed Meteorological Drought Characteristics in China from 1961 to 2017

Bin Ma [a], Bo Zhang [a,*], Lige Jia [a,b], Hao Huang [a]

[a] College of Geography and Environmental Science, Northwest Normal University, Lanzhou 730070, China

[b] Turism College, Inner Mongolia Normal University, Huhhot 010022, China

## ABSTRACT

Drought is one of the most complex natural disasters, while meteorological drought is the root cause of other types of drought. In this study, all meteorological drought events in China from 1961 to 2017 were calculated using the SPEI of the Julian calendar as a time step. The duration and intensity of meteorological drought events and the major meteorological factors that dominated their development were analyzed and discussed. Our study reveals that the normalized results of the log-logistic distribution almost subject to the standard normal distribution; SPEI-daily can capture more detailed drought process than SPEI-month; The frequency of meteorological drought events in the eastern monsoon area of China is high, the duration is short, and the intensity of drought is weak, while the frequency of drought events the northwest arid region is low, the duration is long, and the intensity is strong; Trend of the drought events' frequency of China from 1961 to 2017 is consistent with the global trend; The dominant factors of drought events by Sobol's global sensitivity analysis revealed that the frequency of drought events dominated by PET in the northwest arid region and southern China decreased from 1961 to 1980, and began to increase after 1990; The characteristics of the changes in China's meteorological drought events that we reveal can not only provide reference for disaster prevention and mitigation, but also provide insights for China to adapt to global climate change.

**Keywords:** SPEI-daily; Drought events; Sensitivity analysis; China

## 1. Introduction

Drought is one of the most serious natural disasters that endanger humans and the environment, and its impact has spread all over the world (Hao et al., 2014; Organization, 2014; Wang et al., 2014). More research indicates that global warming caused by human activities accelerates water-heat balance and exposes more regions of the world to the risk of drought (Kumar et al., 2015; Liu and Allan, 2013; Lu et al., 2007; Marvel et al., 2019). Increased frequency and intensity of droughts cause huge loss of life and property while threatening the safety of global ecosystems (Cook et al., 2014; Schwalm et al., 2017). Therefore, the improvement in drought monitoring capabilities is not only an important measure to mitigate disaster, but also enhances human ability to adapt to climate change.

The ability to provide early warning of a drought's onset, severity, persistence and spatial extent promptly is a critical task for drought monitoring (Hayes et al., 2011). However, the complexity of the drought forming mechanism makes monitoring difficult (Quiring, 2009; Wilhite, 2012). Meteorological drought is also the basis of identifying other drought types (Wilhite and Glantz, 1985; Zwiers et al., 2013). The development of the meteorological drought monitoring indexes had gone through a single factor of the elements, which are based on the principle of water balance (Van Loon et al., 2016; Vicente-Serrano et al., 2018; Wilhite, 2012). Three landmark drought indices have gradually improved people's ability to monitor meteorological droughts: the palmer drought severity index (PDSI) is to use water balance during drought calculations (Palmer, 1965); McKee et al. (1993) invented the standardized precipitation index (SPI) by linking drought frequency of multiple time scales; Vicente-Serrano et al. (2010) defined the standardized precipitation evapotranspiration index (SPEI) after standardizing the water balance, which increased the potential evapotranspiration based on the SPI calculation principle. Indexes mentioned above

are currently the three most widely used meteorological drought index, which original and improved versions have been researched globally (Chen et al., 2019; Dai, 2011; Vicente-Serrano et al., 2012; Zarch et al., 2015). These meteorological drought indexes are adept in monitoring drought processes on a month or longer scales (Vicente-Serrano et al., 2010; Zhao et al., 2017). However, some recent studies have found that extreme weather events are affecting the duration and intensity of drought (Ford and Labosier, 2017; Ford et al., 2015; Hunt et al., 2009; Hunt et al., 2014; Mozny et al., 2012). Precipitation deficit may turn into precipitation surplus due to heavy rainstorms in a few days, which may limit more drought details to be captured by the monthly drought index (Byun and Wilhite, 1999; Zhang et al., 2018). Therefore, the time resolution of meteorological drought monitoring needs to be improved.

The choice of the basic unit time of drought monitoring is a controversial issue. The base time unit for the data entered during SPEI calculations is month or week, which is based on Thornthwaite's experiment (Thornthwaite, 1948; Vicente-Serrano et al., 2010). However, the moving time window for input data selection in the experiment is the daily scale, rather than the calendar month or week that appears in some investigations. Some studies used daily time steps as the base time units for input data, which were flawed in some details. In Europe, Stagge et al. (2015) discussed the effect of different probability distributions on SPEI calculations for daily time steps, but it did not analyze whether droughts that have occurred can be captured by drought index. Some SPEI studies in China on daily time steps were parameters that use the plotting position to estimate the probability-weighted moment (Jia et al., 2018; Wang et al., 2016; Wang et al., 2015), while Beguería et al. (2014) found that the probability-weighted moment parameter using unbiased estimate is better than the plotting position. Therefore, choosing the right time step and reasonable

conditional distribution are the key to accurate capture of drought signal by SPEI. Consequently, we will discuss the effect of appropriate conditional distribution on the normalized results, and then analyze the ability of the SPEI index to capture drought signals at different time steps. At the same time, the duration, intensity and changes of the dominant meteorological elements of all drought events in China from 1961 to 2017 will be analyzed.

## 2. Data and methodology

### 2.1 Climate data

The datasets of daily precipitation (mm), maximum and minimum temperature (℃), average relative humidity (%), average wind speed(m/s), sunshine duration, from 839 stations are collected from the Chinese Meteorological Administration (http://data.cma.cn/), covering the period from 1960 to 2017. The measurement height of the wind speed is 10 meters above the ground, and other meteorological elements are obtained from the thermometer screen at 1.5 meters above the ground. Among them, 699 meteorological stations lacked less than 5% of the elements (Fig. 1). We used the stepwise regression analysis to estimate the meteorological elements of the missing data using the data onto the surrounding meteorological stations. At the same time, the quality matching adjustment method (Wang et al., 2007; 2008; 2014) was used to adjust the error of the missing data.

[Fig. 1]

### 2.2 Estimation of potential evapotranspiration

Water balance is the core of the standardized precipitation evapotranspiration index, which is obtained from precipitation minus potential evapotranspiration (PET) (Vicente-Serrano et al., 2010). Precipitation can be obtained directly from observational data, while PET needs to be estimated based on the formula recommended by Food and Agriculture Organization of the United Nations

(FAO) (Allen et al., 1998). The formula for PET is as follows:

$$PET = \frac{0.408\Delta(R_n - G) + \gamma \frac{900}{T_2 + 273} U_2 (e_s - e_a)}{\Delta + \gamma(1 + 0.34U_2)} \quad (1)$$

where $\Delta$ is slope vapour pressure curve [kPa °C$^{-1}$], $\gamma$ is psychometric constant [kPa °C$^{-1}$]; $G$ is the soil heat flux density [MJ m$^{-2}$ day$^{-1}$], when the calculated time step is less than 10 days, it can be ignored; $T_2$ is the mean daily air temperature at 2 meters height [°C], and this study uses data at 1.5 meters high instead; $e_s$ is the saturation vapour pressure [kPa]; $e_a$ is the measured vapour pressure [kPa]; $e_s - e_a$ is saturation vapour pressure deficit [kPa], the $e_s$ and $e_a$ are as follows:

$$e_s = \frac{e^0(\mathrm{T_{max}}) + e^0(\mathrm{T_{min}})}{2} \quad (2)$$

$$e_a = e^0(\mathrm{T_{mean}}) \frac{RH_{mean}}{100} \quad (3)$$

$e^0(\mathrm{T_{max}})$ is the saturation vapour pressure at the mean daily maximum air temperature [kPa]; $e^0(\mathrm{T_{min}})$ is the saturation vapour pressure at the mean daily minimum air temperature [kPa]; $RH_{\mathrm{mean}}$ is the mean relative humidity [%]; $R_{\mathrm{n}}$ is the difference between the incoming net shortwave radiation ($R_{\mathrm{ns}}$) and the outgoing net longwave radiation ($R_{\mathrm{nl}}$) [MJ m$^{-2}$ day$^{-1}$], the formula for $R_{\mathrm{n}}$ is as follows:

$$R_n = R_{ns} - R_{nl} \quad (4)$$

The estimation method of $R_{\mathrm{ns}}$ and $R_{\mathrm{nl}}$ is in Allen's literature (Allen et al., 1998). Solar radiation ($R_s$) is a variable in the calculation $R_{\mathrm{n}}$ formula, which can be calculated by the Angstrom formula (Prescott, 1940). The Angstrom formula is as follows:

$$R_s = \left(a_s + b_s \frac{n}{N}\right) R_a \quad (5)$$

where $n$ is the actual duration of sunshine [hour]; N is the maximum possible duration of sunshine or daylight hours [hour]; Ra is extraterrestrial radiation [MJ m$^{-2}$ day$^{-1}$]; $a_s$ and $b_s$ are empirical

coefficients with recommended values of 0.25 and 0.50. $U_2$ is the wind speed at 2 meters height [m $s^{-1}$], this study uses the recommended formula (equation 4) to convert the wind speed at 10 meters:

$$U_2 = U_z \bullet \frac{4.87}{\ln(67.8 \bullet z - 5.42)} \tag{6}$$

$U_z$ is the measures wind speed at z meters above ground surface [m $s^{-1}$]; z is the height of measurement above ground surface.

2.3 Calculation of standardized precipitation evapotranspiration index

The principle of standardized precipitation evapotranspiration index (SPEI) calculation is a classical rational approximation of water balance after parameter estimation (Vicente-Serrano et al., 2010). Calculation process of water balance and classical rational approximation in this study have not been changed, while the probability distribution and parameter estimation have been discussed for applicability (Beguería et al., 2014; Stagge et al., 2015). A three-parameter log-logistic distributed is used to calculate SPEI because the frequency of water balance accumulation can be well simulated with statistical distributions. Its probability density function (formula 7) and probability distribution function (formula 8) are expressed as:

$$f(x) = \frac{\beta}{\alpha}\left(\frac{x-\gamma}{\alpha}\right)^{\beta-1}\left[1+\left(\frac{x-\gamma}{\alpha}\right)^{\beta}\right]^{-2} \tag{7}$$

$$F(x) = \left[1+\left(\frac{\alpha}{x-\gamma}\right)^{\beta}\right]^{-1} \tag{8}$$

where $\alpha$, $\beta$, and $\gamma$ are scale, shape, and origin parameters, respectively, for $D_i$ values in the range ($\gamma > D_i < \infty$). Three parameters can be estimated by Ahmad et al. (1988) recommended L-moment procedure. The estimated expression of the three parameters is as follows:

$$\beta = \frac{2w_1 - w_0}{6w_1 - w_0 - 6w_2} \tag{9}$$

$$\alpha = \frac{(w_0 - 2w_1)\beta}{\Gamma(1+1/\beta)\Gamma(1-1/\beta)} \tag{10}$$

$$\gamma = w_0 - \alpha\Gamma\left(\frac{1+1}{\beta}\right)\Gamma\left(\frac{1-1}{\beta}\right) \tag{11}$$

where $\Gamma(\beta)$ is the gamma function of $\beta$; $w_s$ is the probability weighted moments of order $s$, which can be estimated by unbiased estimation (Hosking, 1986):

$$w_s = \frac{1}{N}\sum_{i=1}^{N}\frac{\binom{N-i}{s}D_i}{\binom{N-1}{s}} \tag{12}$$

$$\begin{aligned} P &= 1 - F(x) \quad F(x) \le 0.5 \\ P &= 1 - P \quad\quad F(x) > 0.5 \end{aligned} \tag{13}$$

$$W = \sqrt{-2\ln(P)} \tag{14}$$

$$SPEI = W - \frac{c_0 + c_1 W + c_2 W^2}{1 + d_1 W + d_2 W^2 + c_3 W^3} \tag{15}$$

where $N$ is the chosen time scale (daily), and $D_i$ is differential values between precipitation and PET at different time scales. $c_0$ = 2.515517, $c_1$ = 0.802853, $c_2$ = 0.010328, $d_1$ = 1.432788, $d_2$ = 0.189269, $d_3$ = 0.001308. The expressions of Weibull, Pearson-III (P-III), generalized pareto distribution (GPD) and generalized extreme value distribution (GEV) are given in the literature (Stagge et al., 2015; Wang et al., 2019). The division of SPEI drought level refers to the proportion of the area occupied by different SPEI values in the standard normal distribution (Table 1).

[Table 1]

2.4 Quantification of meteorological drought duration

Meteorological drought refers to the phenomenon of atmospheric water deficit due to precipitation deficit in a period (Mishra and Singh, 2010). Therefore, the length of consecutive dry days is an important basis of judging drought events. Although there will be consecutive dry days

during heat waves, meteorological droughts will last longer (Chang and Wallace, 1987). In some studies, a period as short as 15 or 25 days with little rain has been defined as a dry spell (Chang and Wallace, 1987; Glickman and Zenk, 2000). However, Byun (1999) believed that the duration of drought progress less than 1 Julian month is not important. Therefore, in this study, the threshold of the drought process was defined with a duration of SPEI <-0.5 not less than 30 days.

2.5 Defining drought intensity

Drought intensity is the mean of the drought index during a drought process (Dracup et al., 1980). In this study, we used the intensity of mild, moderate, severe or extreme drought in 30 days as the threshold for dividing the drought intensity. Drought intensity can be expressed as:

$$DI = \left| \frac{1}{n} \sum_{i=1}^{n} SPEI_i \right| \tag{16}$$

where $DI$ is the intensity of a drought process; $n$ is the duration of a drought process, which refers to the duration from drought to the end, not a fixed period of time.

[Table 2]

2.6 Verification of standard normal distribution

Since SPEI is calculated using the classical approximation, the result is only approximated by the standard normal distribution. Therefore, we use Z-test directly to verify that the normalized results subject to the standard normal distribution. Z-test is a hypothesis test used to verify that data is subject to a standard normal distribution. The Z-test in this study was implemented in MATLAB, where the scalar value in the range is 0.05. Detailed algorithms and formulas are available in the literature (Cornell and John, 1971).

2.7 Sobol's global sensitivity analysis

Sobol's global sensitivity is used for estimating the influence of individual variables or groups

of variables on the model output (Sobol, 2001). Sobol's global sensitivity was used in this study to calculate the sensitivity of precipitation and potential evapotranspiration changes to drought events. The calculation procedure of the global sensitivity is as follows:

1. Sobol sequence the independent variable according to the range of the independent variable. The calculation process of Sobol sequences refers to the literature (Sobol, 2011). Since the thresholds of precipitation and potential evapotranspiration are different in each drought event, the selection of sampling thresholds in this study is not described in detail.

2. Constructing sensitivity relationships using independent variables and variances of variables derived from Sobol sequences. The detailed formula is as follows:

$$S_i = \frac{V_i}{\mathrm{Var}(Y)} \tag{17}$$

Where *Si* a direct variance-based measure of sensitivity; *Vi* refers to other terms in the variance decomposition other than the independent variable; Var(*Y*) is the variance of the variable Y.

3. Determination of dominant factors. Sort the sensitivity of each independent variable from the largest to smallest. The independent variable with the largest sensitivity value is the dominant factor of the model.

## 3. Result

### 3.1 Selection of SPEI distribution function

It is a controversy to choose the appropriate probability distribution function in the process of calculating SPEI. It is worth not that the calculation result of SPEI is a normalized process of normalization. Therefore, we should check whether the SPEI results are subject to the standard normal distribution. In this study, we performed standard normal distribution verification on the results after standardization concerning five distribution functions (Weibull, Pearson-III, Log-

Logistic, Generalized Pareto Distribution, and Generalized Extreme Value Distribution). Fig. 2 reveals the Z-test hypothesis test results from five distributed SPEI results using plotted position (pp) and unbiased estimation (ub) for parameter estimation. The results of the Weibull and P-III distributions normalized in Fig. 2 a 1-4 and b 1-4 are hardly normalized normal distributions. The GPD (Fig. 2 d 1-4) have standard normal distribution only at pp-month, and the other results almost reject the hypothesis test. In GEV (Fig. 2 c 1-4), the results of ub-daily are normalized normal distribution, and the other three results to reject the hypothesis test. In the log-logistic distribution, there are very few stations that fail to reject the hypothesis test of the results of ub-month and pp-month, while the SPEI with daily as the step sizes subject to the normalized normal distribution. Among all the standardized results, only all sites in ub-Log, pp-Log, and ub-GEV with daily as the time step are standardized positive distribution. The normalized results of the classical approximation are only approximate to the standard normal distribution. Therefore, the choice of the optimal distribution needs to discuss the variation on the mean and standard deviation. The mean and standard deviation from the normalized results of all distributions is listed in Table 3. The results of the log-logistic distribution in Table 3 with daily time steps are closest to the standard normal distribution (mean=0, standard deviation=1). Although all stations in ub-GEV-daily in Fig. 2 e1 did not reject the hypothesis test, their mean and standard deviation indicate that they are not very close to the standard normal distribution. The above analysis has revealed that the normalized results of the log-logistic distribution almost subject to the standard normal distribution.

[Fig. 2]

[Table 3]

Ten sites with meteorological drought disaster records in this study were randomly selected

concerning different climatic regions. The drought records of these stations are from the *Statistical Yearbook of the China Meteorological Administration*. The distribution selected when calculating SPEI in Fig. 3 are ub-Log-daily and ub-Log-month. Fig. 2 reveals that SPEI-month and SPEI-daily have the same drought trend in almost stations. SPEI-daily of 10 weather stations can almost capture drought signals matching the meteorological drought disaster records. In August 2017, meteorological drought at station 53446 (Baotou) has been alleviated, while SPEI-month is monitoring extreme drought. SPEI-month underestimated meteorological drought signal during extreme drought at 54454 (Qamdo) station from April to July 2017. A brief extreme drought occurred at the 57805 (Zhijin) station in August 2017, but SPEI-month detected that the drought started in July. Except for these three cases, SPEI-month of other stations have detected drought signals similar to SPEI-daily. The results of the comparison reveal that heavy rainstorms in the short term will affect the monitoring effect of SPEI-month. The drought processes and intensity revealed by SPEI-daily are almost consistent with the artificial drought record.

[Fig. 3]

3.2 Spatial distribution of the drought events' frequency

In this study, the threshold of the drought process was defined with a duration of SPEI <-0.5 not less than 30 days. The frequency of drought events that have occurred in China is gradually reduced from the southeast coast to the northwest inland as shown in Fig. 4a. The region with the highest drought events' frequency in China has a frequency of more than 80, mainly distributed in South China. The areas with the fewest occurrences of drought events are distributed in the northwest arid region. The frequency of occurrences of drought events is consistent with the distribution of the isohyet (Lu et al., 2019).

[Fig. 4]

In this study, drought processes with durations of 30-60 days (1-2 months), 60-90 days (2-3 months), and greater than 90 days (>3 months) are counted in Fig. 4 b, c, d. The maximum frequency of drought events lasting 30-60 days in the south of the eastern monsoon area exceeded 50, while the frequency of the event occurred in the northwest arid region are less than 20 (Fig. 4 b). The frequency of drought events lasting between 60-90 days are low in China, and few sites have frequencies exceeding 30. The frequency of drought events lasting more than 90 days in the arid regions of northwest China is more than 40, while in the eastern monsoon region the frequency of the event are less than 20. Meanwhile, the frequency of drought events in different durations appearing in six different decades are expressed in Fig. S.1. The supplementary Fig. S.1 a1-5 reveal that the frequency of all drought events in eastern China have decreased during the 1960s-1980s and has increased since the 1990s, especially in South China. We find that the duration of drought is shorter in the eastern monsoon region where the frequency of drought events is higher, and the duration of the drought is longer in the northwest arid region where the frequency of drought events is lower.

3.3 Spatial distribution of drought events with different intensities

Referring to the classification criteria of SPEI drought severity in Table 2 the drought intensity (DI) in the study is divided into four levels: DI ≤ 30 ($DI_{30}$), 30 < DI ≤45 ($DI_{30-45}$), 45< DI ≤ 60 ($DI_{45-60}$), and DI >60 ($DI_{60}$). These four types of drought intensity indicate the cumulative amount of mild, moderate, severe or extreme drought events within a water balance period (30 days). Referring to Table 2, the four types of drought intensity are 15, 30, 45 and 60 respectively. Different levels' frequency of drought intensity as a percentage of all drought events are plotted in Fig. 5. The

proportion of $DI_{30}$ in the eastern monsoon region is higher than that in the northwest arid region (Fig. 5 a). Its high-value area is distributed in the middle and lower reaches of the Yangtze River, and the low-value area is in the hyper-arid zone area. $DI_{30-45}$ and $DI_{45-60}$ account for less than 20% in the eastern region and less than 10% in the arid regions of the northwest (Fig. 5 b, c). $DI_{60}$ shows the opposite trend of $DI_{30}$, that is, the northwest arid region is high, and the east is low. Meanwhile, we also found that the proportion of events with extreme intensity is high in the northwest arid region, and the regions with high proportions of mild intensity are concentrated in the eastern monsoon region. The same regularity as the frequency distribution of drought events of different durations is also found in the Fig. S. 2. The intensity of the 1960s-1980s drought was decreasing, but the intensity increased after 1990s. Especially after 2000, the coverage of $DI_{30}$ and $DI_{60}$ in the eastern monsoon exceeded the previous four decades.

[Fig. 5]

After analyzing the frequency of drought events with different durations and intensity, we found that the drought events in the northwest arid region with a low frequency of drought events have a long duration and high intensity, while those in the eastern monsoon region with high frequency of drought events have a short duration and low intensity. The frequency and intensity of drought events that had occurred in eastern China have gradually declined in the 1960s-1980s, and have risen since 1990. Besides, in the area bordered by Yunnan Province and Sichuan Province, where the average precipitation for many years exceeds 800 mm, the drought event here has a long duration and high intensity.

3.4 Impact of changes in precipitation and PET on drought events

Sobol's global sensitivity principle (Sobol, 2001) is used to calculate the sensitivity of

precipitation and PET to drought events. The frequency of drought events dominated by PET in Fig. 5a decreases from southeast to northwest. More than 45 drought events dominated by PET in the south of 30 ° N and east of 105 ° E. The frequency of PET-dominated drought events in the northwest arid region ranges between 35-45. Less than 30 drought events triggered by PET in the northwest arid region. The frequency of drought events caused by precipitation deficits is less than 30 in the eastern monsoon region, the Yangtze River Basin, and the Huaihe River Basin (Fig. 5b). In the northwest arid region, the border between Yunnan and Sichuan, the frequency of drought events induced by precipitation deficits are higher than 30. In general, the frequency of drought events induced by PET is greater than the precipitation deficit in the eastern monsoon region, while the frequency of drought events induced by precipitation deficit in the northwest arid region is higher than that caused by PET.

[Fig. 5]

The frequency of drought events induced by precipitation and PET in different decades are plotted in Fig. S. 3 to reveal the variation in drought events' frequency dominated by different meteorological elements in China from 1961 to 2017. The proportion of drought events in Supplementary Figure S.3a indicates that the proportion of drought events in the South China caused by PET was the highest in 1961-1990, showing a gradual decrease trend, and then gradually increasing after 1991. The proportion of drought events caused by precipitation deficits gradually decreased in the arid regions of the northwest from 1961 to 1990, and then increased from 1991 to 2000, and then gradually decreased. (Fig. S. 3b).

**4. Discussion**

SPEI is one of the more applicable meteorological drought monitoring indexes, which has been

recognized in many studies in different regions of the world (Byakatonda et al., 2018; Chen et al., 2019; Huimean et al., 2018; Song et al., 2015). However, the choice of conditional distribution has always been the main problem of scholars' controversy (Stagge et al., 2015; 2016; Vicenteserrano and Begueria, 2016; Wang et al., 2019). Previous researchers ignored that only the drought threshold defined by the probability distribution function when the standardized results must subject to or approximate the standard normal distribution is statistically significant (Vicente-Serrano et al., 2010). In this study, we verified the normalized results using the Z-test to find that the log-logistic distribution is the best conditional distribution. As revealed in the Stagge et al. (2015) and Wang et al. (2019) studies, other distributions have followed the normal distribution before standardization, but the standardized result is not the standard normal distribution. Our study also found that the results normalized using the classical approximation method only approximate the standard normal distribution, although the error is very small. Therefore, choosing the appropriate conditional distribution under different standardized methods will be one of the focuses of our future research.

The choice of calculating the basic time step size of SPEI is also a question worth discussing. When discussing the choice of the conditional distribution, we find that the normalized results of the log-logistic distribution almost subject to the standard normal distribution. To reveal the difference in droughts between SPEIs at different time steps, this study randomly selected 10 meteorological stations with meteorological drought disaster records in different climatic regions. The results of the comparison found that SPEI-daily and SPEI-month have similar results in monitoring the trend of drought events. SPEI-daily can reveal more drought events details than SPEI-month.

The studies on meteorological drought index in China mostly involve the dry and wet changes

of regional climate caused by the cumulative effect of drought events (Huimean et al., 2018; Lu et al., 2019; Song et al., 2015). In this study, we revealed the frequency and intensity of drought events in China from 1961 to 2017. The studies by Wang et al. (2016) and Zhang et al. (2019) revealed that the frequency of flash droughts in China is increasing after the 1980s, but the change between 1960 and 1980 was not revealed by them. In addition to the same change laws after the 1980s, our research also reveals that the frequency of drought in China is decreasing from 1961 to 1980, which is consistent with the trend of the frequency change of global drought events by Marvel et al. (2019). The highest proportion of drought events with drought intensity exceeding $DI_{90}$ is in the northwest arid region. However, these meteorological drought events are often easily transformed into climate drought. In addition to this, drought events with a severity exceeding $DI_{90}$ in other regions maintained a low proportion. Comparing the proportion of drought events with different intensities, we can find that the definition of drought intensity in this study is reasonable.

Water deficit determined by precipitation and ET a direct cause of meteorological drought (Wang and Yuan, 2018). The frequency of PET-related drought events is decreasing in our study, especially in the northwest arid and south of China's monsoon region from 1961 to 1980. However, some studies have found that the PET in the area matching our research has decreased after the 1960s (Fan et al., 2016; Yin et al., 2010). Although only the sensitivity at the time of drought was analyzed in our study, we found that the change in the frequency of PET-sensitive drought events is similar to the global PET change trend, indicating that the PET-sensitive drought events in China are still related to long-term changes in the global climate. The fluctuation of the frequency of drought events caused by precipitation in the northwest arid region after the 1990s is closely related to the increase in precipitation, but this has not changed the long-term climate drought.

## 5. Conclusions

The z-test test reveals that the log-logistic distribution fitting results almost subject to the standard normal distribution. Compared with randomly selected drought events, SPEI-daily is superior to SPEI-month in monitoring the occurrence of drought.

The frequency of drought events in China from 1961 to 2017 decreased from southeast to northwest, with high-value areas concentrated in southern China and low-value areas distributed in the northwest arid region. The duration of the drought event in the eastern monsoon area is usually less than three months, while that in the northwest arid area is more than three months. The frequency of drought events in China is consistent with the global change trend, that is, it gradually declined from 1961 to 1980, and continued to increase thereafter.

Statistic of the intensity of drought events found that the intensity of drought in the eastern monsoon area with a large number of events was low, while that in the northwest arid region with few events was high. The frequency and intensity of drought events that had occurred in eastern China have gradually declined in the 1960s-1980s, and have risen since 1990.

Sobol's global sensitivity principle reveals that the frequency of PET-induced drought events is greater than the precipitation deficit in the eastern monsoon, but the frequency of drought events dominated by precipitation is higher than that of PET in the northwest arid region. The high-value areas of the frequency of drought events induced by PET are distributed in the southern region, and the low-value areas of the frequency of events induced by precipitation deficit are in the Yangtze River Basin.

## Acknowledgements

This study was financially supported by the National Natural Science Foundation of China (No. 41561024, No. 31760241, No. 41801054)

## Reference

Ahmad M I, Sinclair C D, Werritty A, 1988. Log-logistic flood frequency analysis. Journal of Hydrology. 98(3-4): 205-224. http://doi.org/10.1016/0022-1694(88)90015-7.

Allen, R.G., Pereira, L.S., Raes, D. et al., 1998. Crop evapotranspiration-Guidelines for computing crop water requirements-FAO Irrigation and drainage paper 56. 300, D05109.

Begueria S, Vicente-Serrano S M, Reig F et al., 2014. Standardized precipitation evapotranspiration index (SPEI) revisited: parameter fitting, evapotranspiration models, tools, datasets and drought monitoring. International Journal of Climatology. 34(10): 3001-3023. http://doi.org/10.1002/joc.3887.

Byakatonda J, Parida B P, Moalafhi D B et al., 2018. Analysis of long term drought severity characteristics and trends across semiarid Botswana using two drought indices. Atmospheric Research. 213(7): 492-508. http://doi.org/10.1016/j.atmosres.2018.07.002.

Chen S, Gan T Y, Tan X Z et al., 2019. Assessment of CFSR, ERA-Interim, JRA-55, MERRA-2, NCEP-2 reanalysis data for drought analysis over China. Climate Dynamics. 53(1-2): 737-757. http://doi.org/10.1007/s00382-018-04611-1.

Cook B I, Smerdon J E, Seager R et al., 2014. Global warming and 21st century drying. Climate Dynamics. 43(9-10): 2607-2627. http://doi.org/10.1007/s00382-014-2075-y.

Cornell, John A, 1971. Introductory Mathematical Statistics: Principles and Methods. Technometrics. 13(4): 922-925.

Dai A G, 2011. Characteristics and trends in various forms of the Palmer Drought Severity Index during 1900-2008. Journal of Geophysical Research Atmospheres. 116(D12115): 1-26. http://doi.org/10.1029/2010jd015541.

Dracup J A, Lee K S, Paulson E G, 1980. On the statistical characteristics of drought events. Water Resources Research. 16(2): 289-296. http://doi.org/10.1029/WR016i002p00289.

Fan J L, Wu L F, Zhang F C et al., 2016. Climate change effects on reference crop evapotranspiration across different climatic zones of China during 1956-2015. Journal of Hydrology. 542(11): 923-937. http://doi.org/10.1016/j.jhydrol.2016.09.060.

Ford T W, Labosier C F, 2017. Meteorological conditions associated with the onset of flash drought in the Eastern United States. Agricultural and Forest Meteorology. 247(12): 414-423. http://doi.org/10.1016/j.agrformet.2017.08.031.

Ford T W, McRoberts D B, Quiring S M et al., 2015. On the utility of in situ soil moisture observations for flash drought early warning in Oklahoma, USA. Geophysical Research Letters. 42(22): 9790-9798. http://doi.org/10.1002/2015gl066600.

Hao Z C, AghaKouchak A, Nakhjiri N et al., 2014. Global integrated drought monitoring and prediction system. Scientific Data. 1(2014): 140001. http://doi.org/10.1038/sdata.2014.1.

Hayes M, Svoboda M, Wall N et al., 2011. The Lincoln Declaration on Drought Indices: Universal Meteorological Drought Index Recommended. Bulletin of the American Meteorological Society. 92(4): 485-488. http://doi.org/10.1175/2010bams3103.1.

Hosking JRM, (1986). The theory of probability weighted moments. Res. Rep. RC 12210 IBM Research Division, Yorktown Heights NY 10598.

Huimean F, Yusop Z, Yusof F, 2018. Drought analysis and water resource availability using standardised precipitation e vapotranspiration index. Atmospheric Research. 201(3): 102-115. http://doi.org/10.1016/j.atmosres.2017.10.014.

Hunt E D, Hubbard K G, Wilhite D A et al., 2009. The development and evaluation of a soil moisture index. Interna tional Journal of Climatology. 29(5): 747-759. http://doi.org/10.1002/joc.1749.

Hunt E D, Svoboda M, Wardlow B et al., 2014. Monitoring the effects of rapid onset of drought on non-irrigated mai ze with agronomic data and climate-based drought indices. Agricultural and Forest Meteorology. 191(2014): 1-11. http://doi.org/10.1016/j.agrformet.2014.02.001.

Jia Y Q, Zhang B, Ma B, 2018. Daily SPEI Reveals Long-term Change in Drought Characteristics in Southwest Chin a. Chinese Geographical Science. 28(4): 680-693. http://doi.org/10.1007/s11769-018-0973-3.

Kumar S, Allan R P, Zwiers F et al., 2015. Revisiting trends in wetness and dryness in the presence of internal clima te variability and water limitations over land. Geophysical Research Letters. 42(24): 10867-10875. http://doi.org/10. 1002/2015gl066858.

Liu C L, Allan R P, 2013. Observed and simulated precipitation responses in wet and dry regions 1850-2100. Environ mental Research Letters. 8(3): 1-11. http://doi.org/10.1088/1748-9326/8/3/034002.

Lu J, Vecchi G A, Reichler T, 2007. Expansion of the Hadley cell under global warming. Geophysical Research Letter s. 34(6): 5. http://doi.org/10.1029/2006gl028443.

Lu Y J, Jiang S H, Ren L L et al., 2019. Spatial and Temporal Variability in Precipitation Concentration over Mainla nd China, 1961-2017. Water. 11(5): 16. http://doi.org/10.3390/w11050881.

Marvel K, Cook B I, Bonfils C J W et al., 2019. Twentieth-century hydroclimate changes consistent with human influ ence. Nature. 569(2019): 59-65. http://doi.org/10.1038/s41586-019-1149-8.

McKee, T.B., Doesken, N.J., Kleist, J., The relationship of drought frequency and duration to time scales. Proceedings of the 8th Conference on Applied Climatology, American Meteorological Society Boston, MA (1993), pp. 179-18 3.

Mo K C, Lettenmaier D P, 2016. Precipitation Deficit Flash Droughts over the United States. Journal of Hydrometeoro logy. 17(4): 1169-1184. http://doi.org/10.1175/jhm-d-15-0158.

Mozny M, Trnka M, Zalud Z et al., 2012. Use of a soil moisture network for drought monitoring in the Czech Repu blic. Theoretical and Applied Climatology. 107(1-2): 99-111. http://doi.org/10.1007/s00704-011-0460-6.

Organization, W.M., 2014. Atlas of mortality and economic losses from weather, climate and water extremes (1970-201 2).

Otkin J A, Svoboda M, Hunt E D et al., 2018. Flash droughts: A review and assessment of the challenges imposed b y rapid-onset droughts in the United States. Bulletin of the American Meteorological Society. 99(5): 911-919. http: //doi.org/10.1175/bams-d-17-0149.1.

Palmer, W., Meteorological Drought. Research Paper No. 45, 1965, 58 p, (1965) 1-65 pp.

Prescott J A, 1940. Evaporation from a water surface in relation to solar radiation. Transactions of the Royal Society of South Australia. 46(1940): 114-125.

Quiring S M, 2009. Developing Objective Operational Definitions for Monitoring Drought. Journal of Applied Meteorol ogy and Climatology. 48(6): 1217-1229. http://doi.org/10.1175/2009JAMC2088.1.

Schwalm C R, Anderegg W R L, Michalak A M et al., 2017. Global patterns of drought recovery. Nature. 548(2017): 202–205. http://doi.org/10.1038/nature23021.

Sobol I M, 2001. Global sensitivity indices for nonlinear mathematical models and their Monte Carlo estimates. Mathe matics and Computers in Simulation. 55(1-3): 271-280. http://doi.org/10.1016/s0378-4754(00)00270-6.

Song X Y, Song S B, Sun W Y et al., 2015. Recent changes in extreme precipitation and drought over the Songhua River Basin, China, during 1960-2013. Atmospheric Research. 157(4): 137-152. http://doi.org/10.1016/j.atmosres.201

5.01.022

Stagge J H, Tallaksen L M, Gudmundsson L et al., 2015. Candidate Distributions for Climatological Drought Indices (SPI and SPEI). International Journal of Climatology. 35(13): 4027-4040. http://doi.org/10.1002/joc.4267.

Stagge J H, Tallaksen L M, Gudmundsson L et al., 2016. Response to comment on "Candidate Distributions for Clima tological Drought Indices (SPI and SPEI)'. International Journal of Climatology. 36(4): 2132-2138. http://doi.org/10. 1002/joc.4564.

Svoboda M, LeComte D, Hayes M et al., 2002. The drought monitor. Bulletin of the American Meteorological Society. 83(8): 1181-1190.

Thornthwaite C W, 1948. An approach toward a rational classification of climate. Geographical Review. 38(1): 55-94.

Van Loon A F, Stahl K, Di Baldassarre G et al., 2016. Drought in a human-modified world: reframing drought definit ions, understanding, and analysis approaches. Hydrology and Earth System Sciences. 20(9): 3631-3650. http://doi.or g/10.5194/hess-20-3631-2016.

Vicente-Serrano S M, Begueria S, Lopez-Moreno J I, 2010. A Multiscalar Drought Index Sensitive to Global Warming: The Standardized Precipitation Evapotranspiration Index. Journal of Climate. 23(7): 1696-1718. http://doi.org/10.11 75/2009jcli2909.1.

Vicente-Serrano S M, Begueria S, Lorenzo-Lacruz J et al., 2012. Performance of Drought Indices for Ecological, Agric ultural, and Hydrological Applications. Earth Interactions. 16(2012): 1-27. http://doi.org/10.1175/2012ei000434.1.

Vicente-Serrano S M, Begueria S, 2016. Comment on 'Candidate distributions for climatological drought indices (SPI a nd SPEI)' by James H. Stagge et al. International Journal of Climatology. 36(4): 2120-2131. http://doi.org/10.1002/ joc.4474.

Vicente-Serrano S M, Miralles D G, Dominguezcastro F et al., 2018. Global Assessment of the Standardized Evapotran spiration Deficit Index (SEDI) for Drought Analysis and Monitoring. Journal of Climate. 31(14): 5371-5393. http:/ /doi.org/10.1175/JCLI-D-17-0775.1.

Wang X L, Wen Q H, Wu Y, 2007. Penalized maximal t test for detecting undocumented mean change in climate dat a series. Journal of Applied Meteorology and Climatology. 46(6): 916-931. http://doi.org/10.1175/JAM2504.1.

Wang X L, 2008. Accounting for Autocorrelation in Detecting Mean Shifts in Climate Data Series Using the Penalized Maximal t or F Test. Journal of Applied Meteorology and Climatology. 47(9): 2423-2444. http://doi.org/10.1175/2 008jamc1741.1.

Wang X L, Feng Y, Vincent L A, 2014. Observed Changes in One-in-20 Year Extremes of Canadian Surface Air Tem peratures. Atmosphere-ocean. 52(3): 222-231. http://doi.org/10.1080/07055900.2013.818526.

Wang Q, Shi P, Lei T et al., 2015. The alleviating trend of drought in the Huang-Huai-Hai Plain of China based on t he daily SPEI. International Journal of Climatology. 35(13): 3760-3769. http://doi.org/10.1002/joc.4244.

Wang L, Yuan X, Xie Z et al., 2016. Increasing flash droughts over China during the recent global warming hiatus. S cientific Reports. 6(1): 30571-30571. http://doi.org/10.1038/srep30571.

Wang L, Yuan X, 2018. Two Types of Flash Drought and Their Connections with Seasonal Drought. Advances in At mospheric Sciences. 35(12): 1478-1490. http://doi.org/10.1007/s00376-018-8047-0.

Wang H, Chen Y, Pan Y et al., 2019. Assessment of candidate distributions for SPI/SPEI and sensitivity of drought to climatic variables in China. International Journal of Climatology. 39(11): 4392-4412. http://doi.org/10.1002/joc.608 1.

Wilhite D A, Glantz M H, 1985. Understanding the drought phenomenon: the role of definitions. Water International. 10(3): 111-120. http://doi.org/10.1080/02508068508686328.

Yin Y, Wu S, Chen G et al., 2010. Attribution analyses of potential evapotranspiration changes in China since the 196 0s. Theoretical and Applied Climatology. 101(1): 19-28. http://doi.org/10.1007/s00704-009-0197-7.

Zarch M A A, Sivakumar B, Sharma A, 2015. Droughts in a warming climate: A global assessment of Standardized p

recipitation index (SPI) and Reconnaissance drought index (RDI). Journal of Hydrology. 526(2015): 183-195. http://doi.org/10.1016/j.jhydrol.2014.09.071.

Zhao H, Gao G, An W et al., 2017. Timescale differences between SC-PDSI and SPEI for drought monitoring in China. Physics and Chemistry of The Earth. 102(2017): 48-58.

Zhang Y, You Q, Chen C et al., 2018. Evaluation of Downscaled CMIP5 Coupled with VIC Model for Flash Drought Simulation in a Humid Subtropical Basin, China. Journal of Climate. 31(3): 1075-1090. http://doi.org/10.1175/jcli-d-17-0378.1.

Zhang Y Q, You Q L, Mao G X et al., 2019. Short-term concurrent drought and heatwave frequency with 1.5 and 2.0 degrees C global warming in humid subtropical basins: a case study in the Gan River Basin, China. Climate Dynamics. 52(7-8): 4621-4641. http://doi.org/10.1007/s00382-018-4398-6.

Zwiers, F.W., Alexander, L.V., Hegerl, G.C. et al., Climate extremes: challenges in estimating and understanding recent changes in the frequency and intensity of extreme climate and weather events. Climate Science for Serving Society, Springer (2013), pp. 339-389.

**Ma Bin**: Conceptualization, Methodology, Data curation, Writing- Reviewing and Editing;
**Zhang Bo**: Conceptualization, Methodology, Writing- Reviewing and Editing;
**Jia Lige:** Methodology, Data curation;
**Huang Hao:** Data curation.

Declaration of interests

☒ The authors declare that they have no known competing financial interests or personal relationships that could have appeared to influence the work reported in this paper.

☒The authors declare the following financial interests/personal relationships which may be considered as potential competing interests:

The authors declared that they have no conflicts of interest to this work.

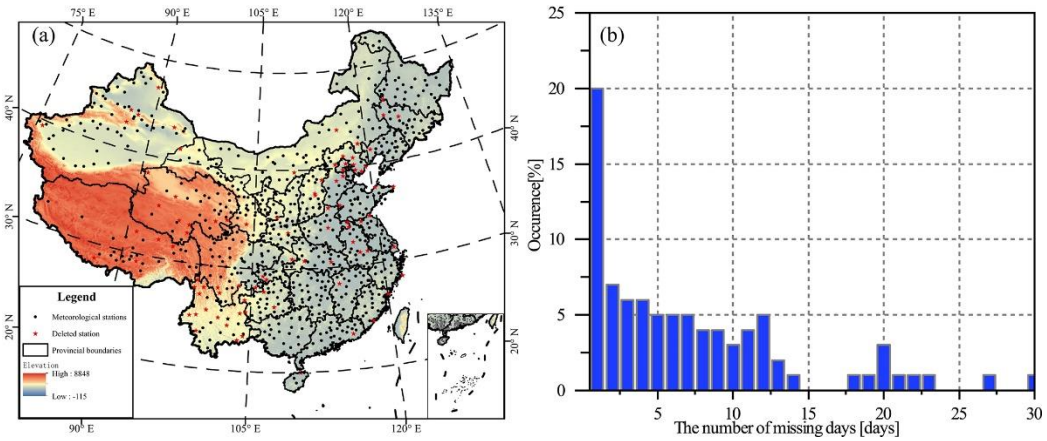


Fig. 1. (a) is the spatial distribution of meteorological stations in China, (b) is the proportion of meteorological stations with missing data.

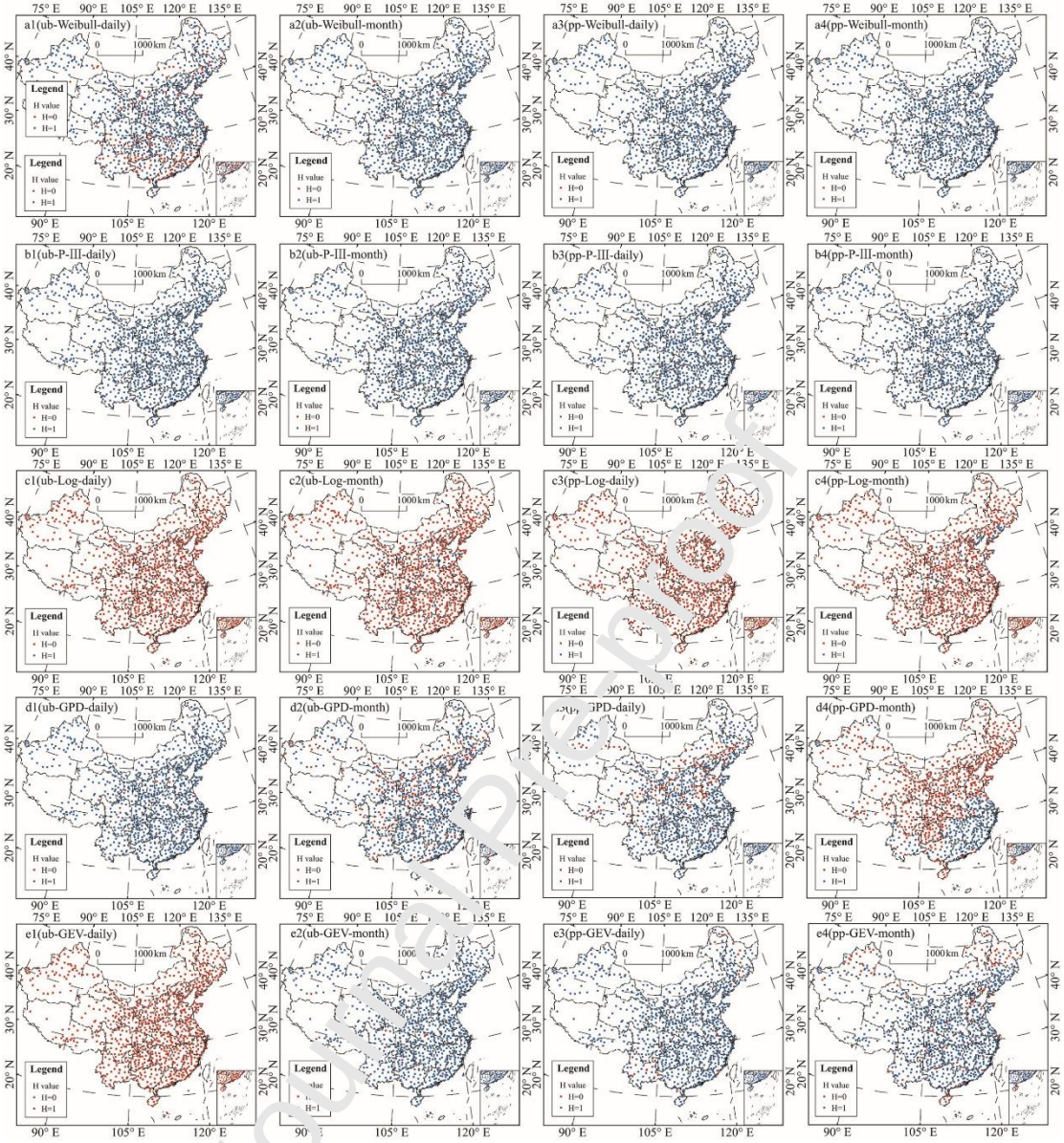


Fig. 2. Spatial distribution of z-test for standardized results in different conditional distributions. a-e is Weibull, Pearson-III (P-III), Log-logistic (Log), generalized pareto distribution (GPD), generalized extreme value distribution (GEV). H=0 means rejecting the null hypothesis at 0.05 significance level; H=1 means that the null hypothesis isn't rejected at the 0.05 significance level.

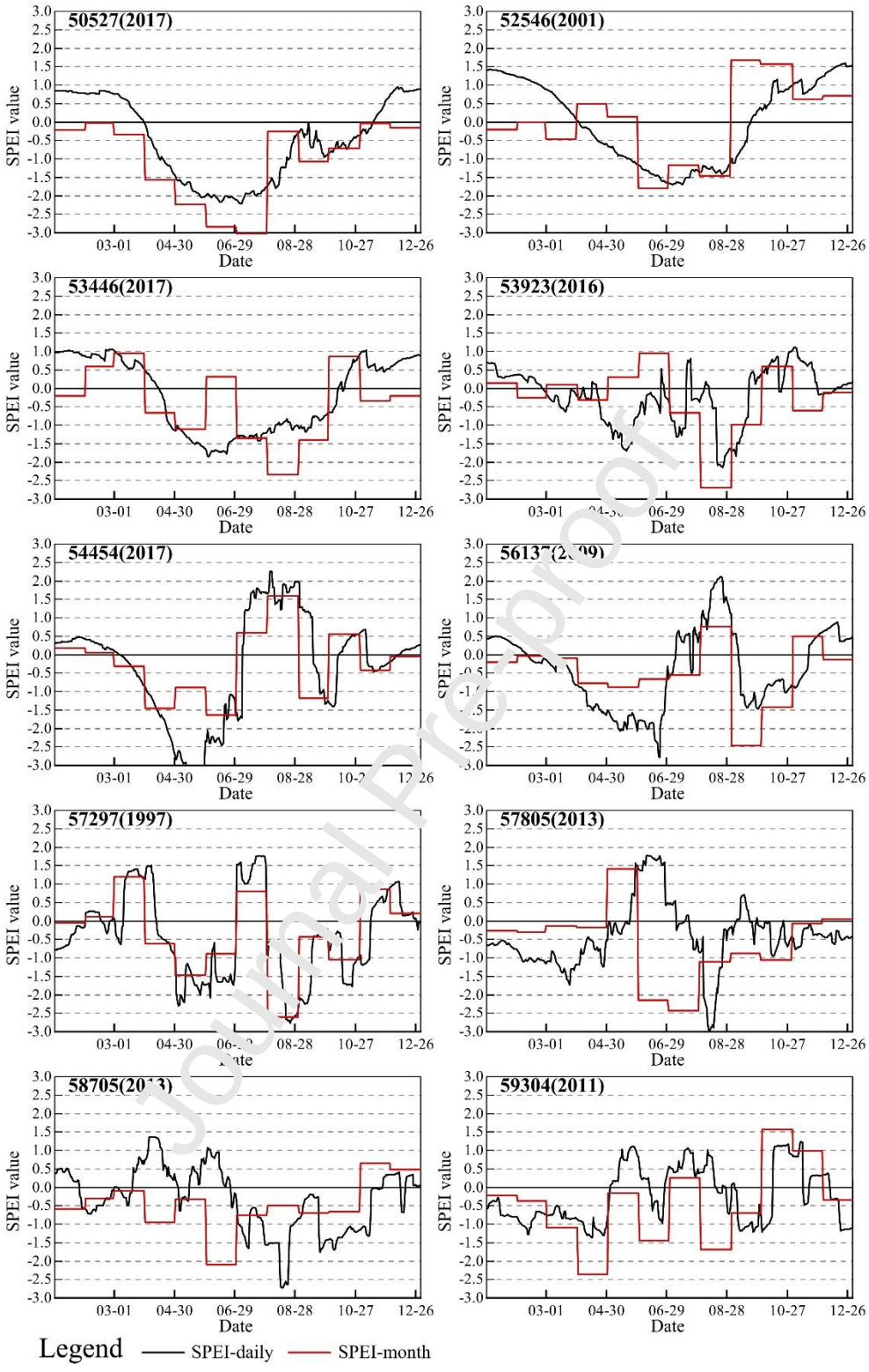


Fig. 3. Comparison of SPEI monitoring drought events at different time steps. 50527 is the weather station ID number, and 2017 is the year in which the meteorological drought event occurred.

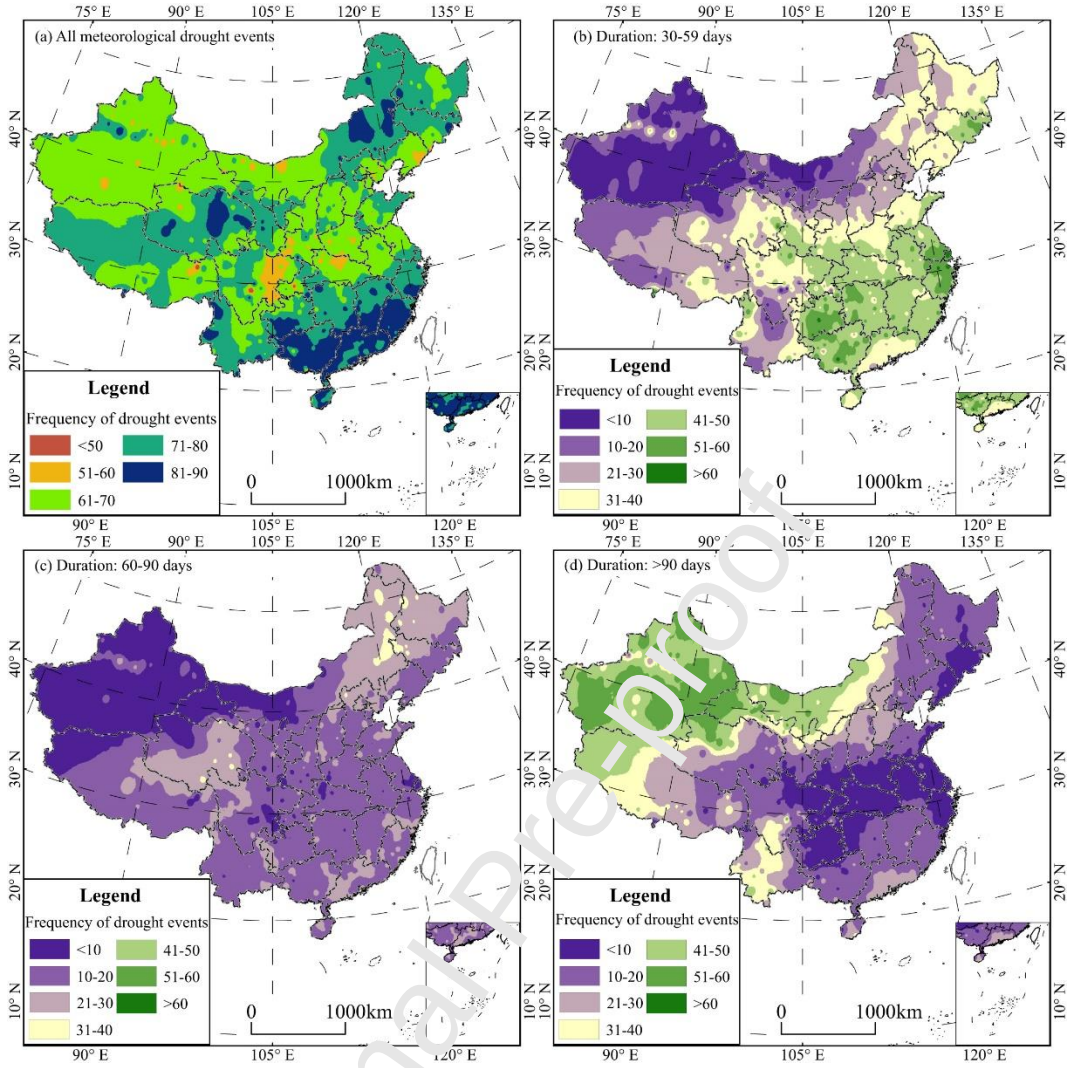


Fig. 4. Spatial distribution of the drought events' frequency with different durations in China from 1961 to 2017. (a) is all meteorological drought events' numbers, (b) is a meteorological drought events lasting 30-59 days, (c) is 60-90 days in duration, and (d) is more than 90 days in duration.

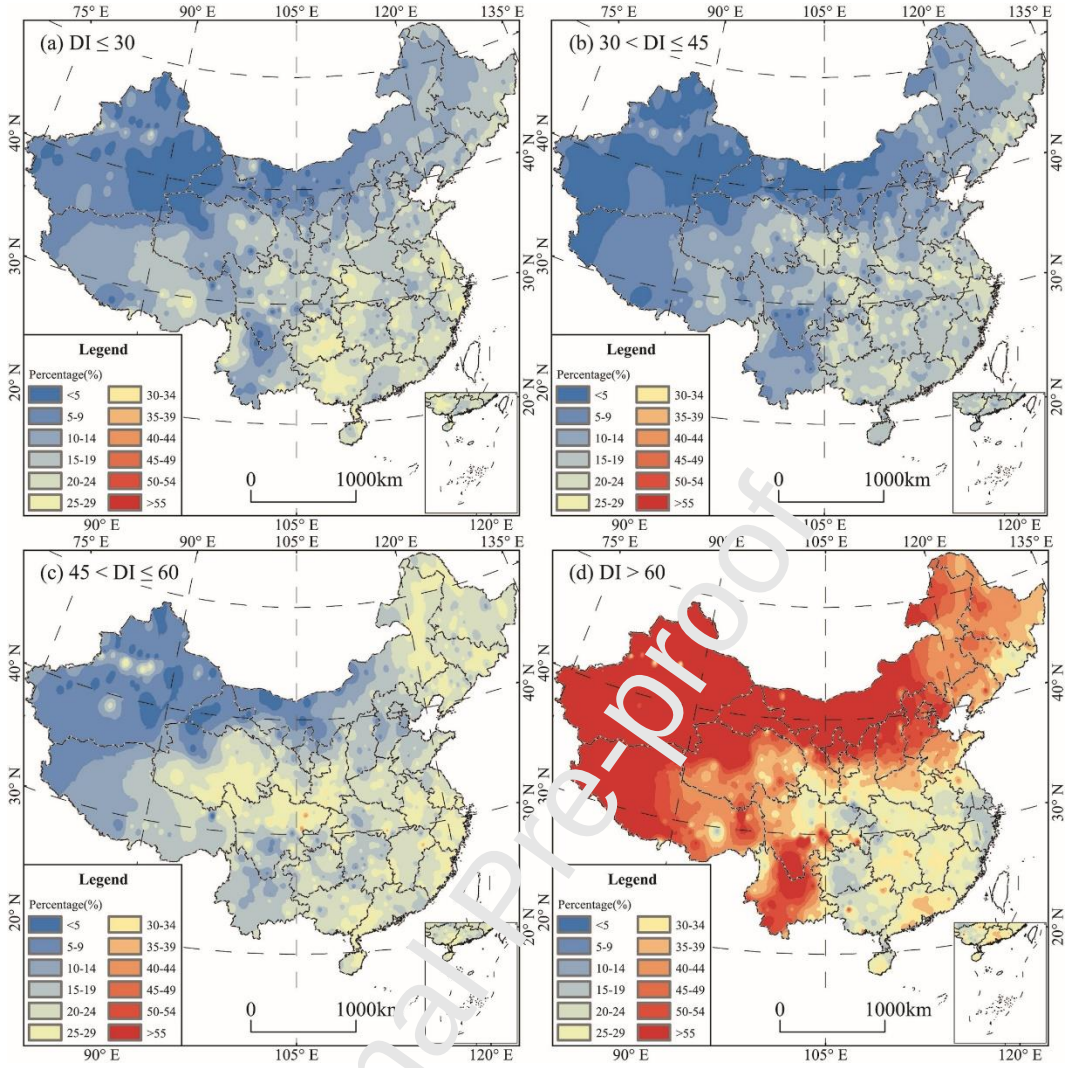


Fig. 5. The proportion of drought events with different drought intensity in all events

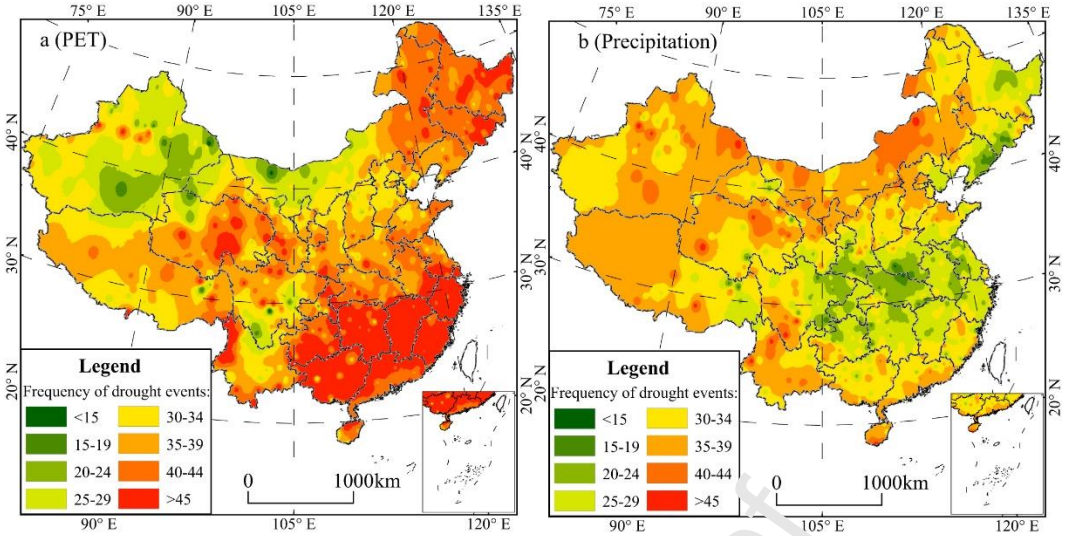


Fig. 6. Spatial distribution of the drought events' frequency dominated by PET and precipitation

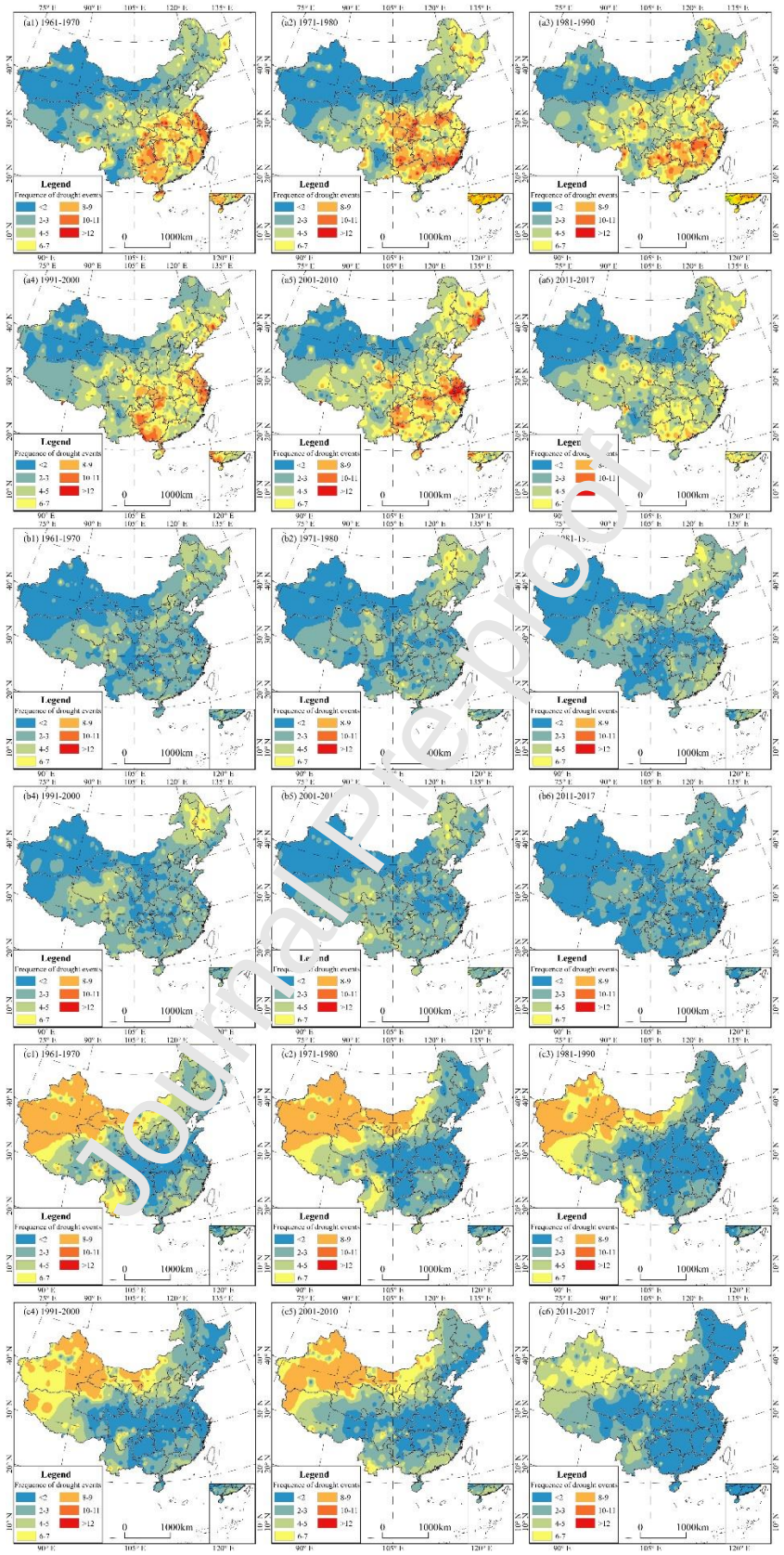


Figure S 1 The spatial distribution of the meteorological drought events' frequency in different decadal in China. (a) is the frequency of all meteorological drought events, (b) is a meteorological drought event lasting 30-59 days, (c) is 60-90 days in duration, and (d) is more than 90 days in duration.

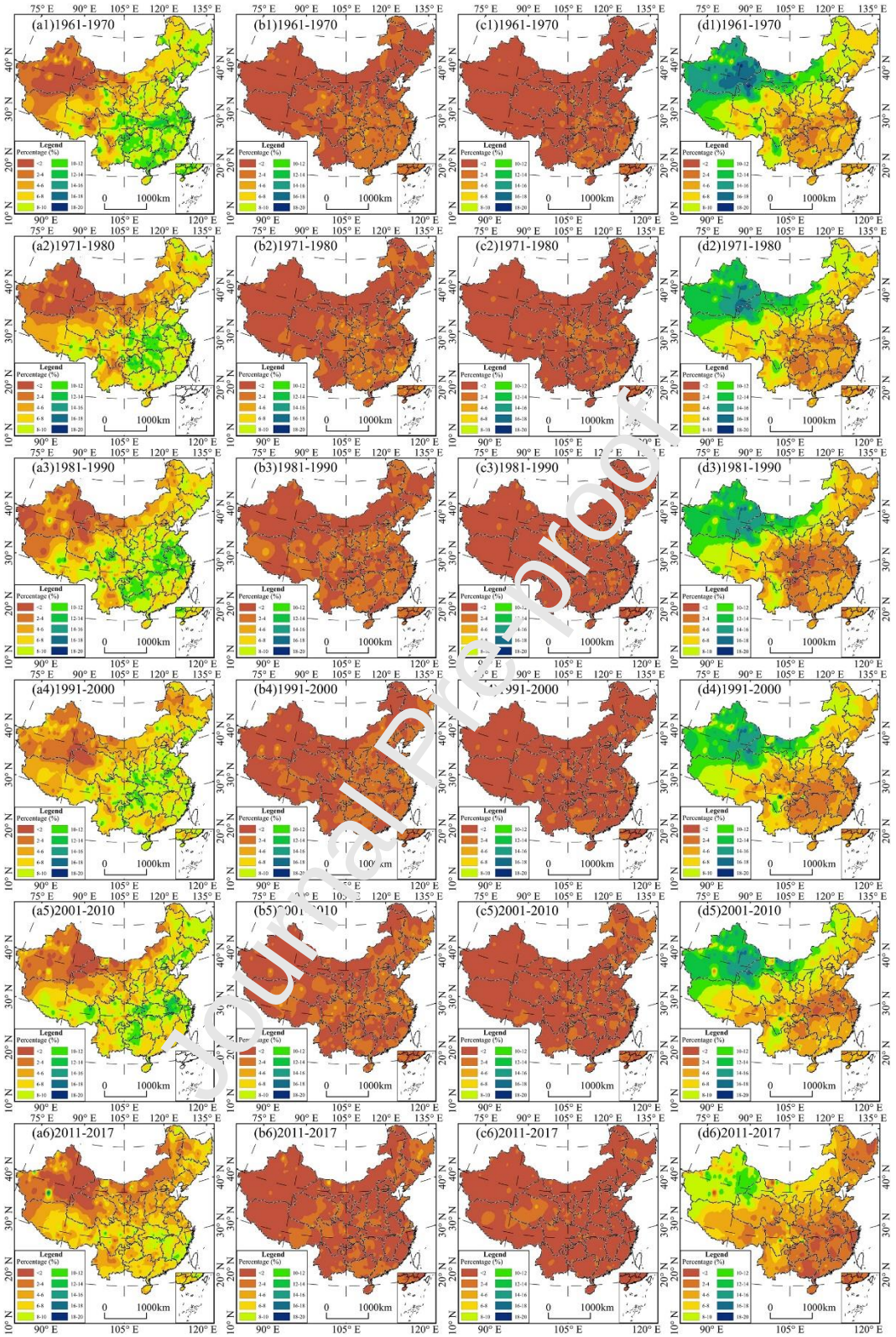


Figure S 2 Spatial distribution of the drought events' proportion with different intensities in different decadal in China. (a) is the frequency of drought events with DI≤30, (b) is the frequency of drought events with 30＜DI≤45, (c) is the frequency of drought events with 45＜DI≤60, and (d) is the frequency of drought events with DI＞60.

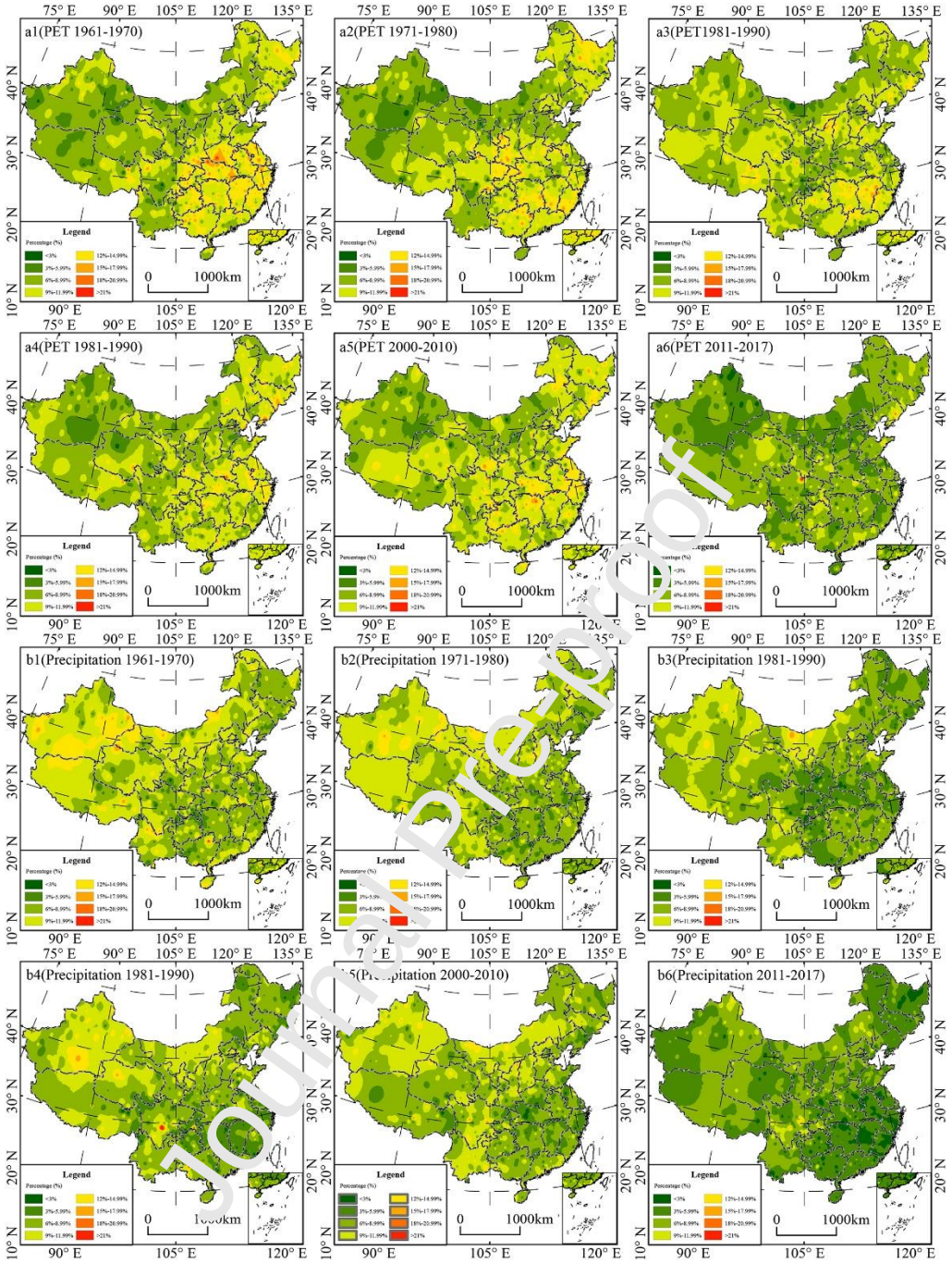


Figure S 3 Spatial distribution of the drought events' frequency dominated by PET and precipitation in different decades.

Table 1 The classification of SPEI values.

| Category | Threshold | Probability Density |
|---|---|---|
| Extremely flood | SPEI>2 | 2.3% |
| Severely flood | 1.5<SPEI≤2 | 4.4% |
| Moderately flood | 1<SPEI≤1.5 | 9.2% |
| Mild flood | 0.5<SPEI≤1 | 14.9% |
| Near normal | -0.5<SPEI≤0.5 | 38.4% |
| Mild drought | -1<SPEI≤-0.5 | 14.9% |
| Moderate drought | -1.5<SPEI≤-1 | 9.2% |
| Severe drought | -2<SPEI≤-1.5 | 4.4% |
| Extreme drought | SPEI≤-2 | 2.3% |

Table 2 Threshold of different drought intensity

| Drought Intensity type | Abbreviation | Drought Intensity (30 day) | SPEI value (mean) |
|---|---|---|---|
| Mild | $DI_{15}$ | 30<DI | -1<SPEI≤-0.5 |
| Moderate | $DI_{30}$ | 30<DI≤45 | -1.5<SPEI≤-1 |
| Severe | $DI_{45}$ | 45<DI≤60 | -2<SPEI≤-1.5 |
| Extreme | $DI_{60}$ | DI>60 | SPEI≤-2 |

Table 3 Mean and standard deviation of normalized values for different conditional distributions

| Distributions | Unbiased Estimation | | | | Plotting Position | | | |
|---|---|---|---|---|---|---|---|---|
| | Mean | | Standard Deviation | | Mean | | Standard Deviation | |
| | daily | month | daily | month | daily | month | daily | month |
| **Weibull** | 0.13 | 0.43 | 0.77 | 2.25 | 0.41 | 0.41 | 2.1 | 2.1 |
| **P-III** | -0.46 | -0.48 | 0.21 | -0.28 | -0.38 | -0.48 | 0.19 | 0.28 |
| **log-logistic** | 0.00 | 0.00 | 1.01 | 1.02 | 0.00 | 0.00 | 1.01 | 1.02 |
| **Generalized Pareto Distributions** | 0.02 | -0.05 | 0.65 | 0.28 | 0.07 | 0.04 | 0.52 | 0.77 |
| **Generalized Extreme Value** | 0.01 | -0.02 | 0.77 | -1.42 | -0.14 | 1.12 | 0.35 | 1.06 |

The highlight of this study are:

The normalized results of the log-logistic distribution almost subject to the standard normal distribution;

SPEI-daily can capture more detailed drought process than SPEI-month;

Trend of the drought events' frequency of China from 1961 to 2017 is consistent with the global trend.